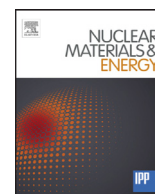


Contents lists available at ScienceDirect

Nuclear Materials and Energy

journal homepage: www.elsevier.com/locate/nme

Density dependence of SOL power width in ASDEX upgrade L-Mode

B. Sieglin*, T. Eich, M. Faitsch, A. Herrmann, D. Nille, A. Scarabosio, ASDEX Upgrade Team

Max-Planck-Institut für Plasmaphysik, Boltzmannstraße 2, D-85748 Garching, Germany

ARTICLE INFO

Article history:

Received 14 July 2016

Revised 14 October 2016

Accepted 15 November 2016

Available online xxx

ABSTRACT

Understanding the heat transport in the scrape-off layer (SOL) and the divertor region is essential for the design of large fusion devices such as ITER and DEMO. Current scalings for the power fall-off length λ_q in H-Mode [1] are available only for the outer divertor target at low densities with low recycling divertor conditions. For the divertor power spreading S only an empirical scaling for ASDEX Upgrade L-Mode is available based on global plasma parameters [2]. Modelling using SOLPS shows a dependence of S on the divertor electron temperature [3]. A more detailed analysis of the heat transport forming λ_q and S is presented for ASDEX Upgrade L-Mode discharges in hydrogen (H), deuterium (D) and helium (He). For low densities the power fall-off length $\lambda_{q,o}$ on the outer divertor target in H and D is described by the same parametric dependencies as the H-Mode scaling [1] but with a larger absolute size of the power fall-off length in L-Mode.

The divertor power spreading S is studied using the local divertor measurements of the target electron temperature $T_{e,tar}$ and density $n_{e,tar}$. It is found that the competition of the diffusive transport parallel and perpendicular to the magnetic field forming $S \propto \sqrt{\chi_{\perp}/\chi_{\parallel}}$ is dominated by the temperature dependence of parallel electron conduction. For high divertor temperatures the ion gyro radius has a significant contribution to S , resulting in a minimum of S at ~ 30 eV.

A recent study [4] with an open divertor configuration found an asymmetry of the power fall-off length between inner and outer target with a smaller power fall-off length $\lambda_{q,i}$ on the inner divertor target. Measurements with a closed divertor configuration find a similar asymmetry for low recycling divertor conditions. It is found, in the experiment, that the in/out asymmetry $\lambda_{q,i}/\lambda_{q,o}$ is strongly increasing with increasing density. Most notably the heat flux density at the inner divertor target is reducing with increasing $\lambda_{q,i}$ whilst the total power onto each divertor target stays constant. It is found that $\lambda_{q,o}$ exhibits no significant density dependence for hydrogen and deuterium but increases with about the square root of the electron density for helium. The difference between H,D and He could be due to the different recycling behaviour in the divertor. These findings may help current modelling attempts to parametrize the density dependence of the widening of the power channel and thus allow for detailed comparison to both divertor effects like recycling or increased upstream SOL cross field transport.

© 2016 The Authors. Published by Elsevier Ltd.

This is an open access article under the CC BY-NC-ND license

(<http://creativecommons.org/licenses/by-nc-nd/4.0/>).

1. Introduction

Understanding and predicting the heat flux profiles on the divertor is mandatory for the development and operation of large fusion devices. So far most of the studies on the target heat load have been carried out on the outer divertor target in low recycling H-Mode conditions. On ASDEX Upgrade recent studies have been conducted to investigate the scrape-off layer and divertor heat transport in low to medium recycling L-Mode conditions. For

the outer divertor target a scaling for the power fall-off length λ_q with similar parametric dependencies as the H-Mode scaling [1] is found which has about twice the absolute magnitude in L-Mode compared to H-Mode. These studies have extended the observation to both the inner and the outer target with an open [4] and closed [5] divertor configuration using high resolution infrared thermography [6]. For both configurations an asymmetry of λ_q between the inner and the outer divertor target has been observed with λ_q being smaller on the inner divertor target compared to the outer divertor target for low recycling conditions. For the closed divertor configuration a density dependence of the in/out asymmetry is observed whereas no density dependence has been observed for the open divertor configuration.

* Corresponding author.

E-mail addresses: Bernhard.Sieglin@ipp.mpg.de, bsieglin@ipp.mpg.de (B. Sieglin).<http://dx.doi.org/10.1016/j.nme.2016.11.011>2352–1791/© 2016 The Authors. Published by Elsevier Ltd. This is an open access article under the CC BY-NC-ND license (<http://creativecommons.org/licenses/by-nc-nd/4.0/>).

Assuming diffusive heat transport in the divertor region and an exponential heat flux profile at the divertor entrance the profile is described by the convolution of the exponential with a Gaussian [1].

$$q(s) = \frac{q_0}{2} \exp\left(\left(\frac{S}{2\lambda_q}\right)^2 - \frac{s}{\lambda_q f_x}\right) \operatorname{erfc}\left(\frac{S}{2\lambda_q} - \frac{s}{Sf_x}\right) \quad (1)$$

Where q_0 is the peak heat flux of the exponential, λ_q is the power-fall off length, S is the width of the Gaussian, f_x is the magnetic flux expansion in the divertor compared to the outer midplane and s is the target coordinate relative to the strike line position. Makowski [7] showed that for this profile shape the effective width λ_{int} is approximated as the sum of λ_q and S .

$$\lambda_{int} \approx \lambda_q + 1.64S \quad (2)$$

For the prediction of the heat load onto the divertor target both λ_q and S need to be understood.

2. Divertor power spreading

The divertor power spreading has been studied in ASDEX Upgrade for L-Mode discharges [2,3,5]. L-Mode conditions were chosen to obtain stable divertor conditions. For the power spreading S in the divertor it was found for the outer target that the increase of S with decreasing target electron temperature $T_{e,tar}$ is due to the strong decrease of parallel electron heat conduction and the resulting higher diffusion time from the divertor entrance to the divertor target [3,5]. For high target temperatures ($T_{e,tar} > 30$ eV) it was found that the ion-gyro radius r_g resulting from the ion heat transport in the sheath has to be taken into account.

$$S = 1.42 \frac{r_g}{f_x} + 2.11 T_{e,tar}^{-1.28} n_{e,tar}^{0.66} A^{-0.84} B_{pol}^{-1.33} \quad (3)$$

Where $T_{e,tar}$ and $n_{e,tar}$ is the electron temperature and density at the divertor target. A is the mass number of the main ion and B_{pol} is the averaged poloidal magnetic field [1].

$$B_{pol} = \frac{\mu_0 I_p}{2\pi a \sqrt{\frac{1+\kappa^2}{2}}} \quad (4)$$

Where I_p is the plasma current, a the minor radius and κ the elongation of the plasma. Assuming that S is originating from a diffusive process the following estimation is done.

$$S = l_x \sqrt{\frac{\chi_{\perp}}{\chi_{\parallel}}} \quad (5)$$

Where l_x is the connection length between the divertor entrance and the target and χ_{\perp} (χ_{\parallel}) is the perpendicular (parallel) heat diffusivity. Assuming electron heat conduction for parallel heat transport the temperature and density dependence are:

$$S = l_x T_e^{-5/4} n_e^{1/2} \sqrt{\frac{\chi_{\perp}}{\kappa_0}} \quad (6)$$

The exponents found for $T_{e,tar}$ and $n_{e,tar}$ with -1.28 and 0.66 are close to the theoretical values -1.25 and 0.5 respectively, expected with parallel electron conductivity and a constant perpendicular heat diffusivity.

To test the limitations of such a power law scaling modelling of heat transport in the divertor region assuming diffusive transport has been performed. These modelling attempts do not include dissipative processes and are only intended to give a qualitative picture on how S changes with changing target electron temperature, they are no substitution for more detailed modelling attempts which include a more complete set of physical processes [8–10]. Fig. 1 shows exemplary results of the modelling attempts. It is seen

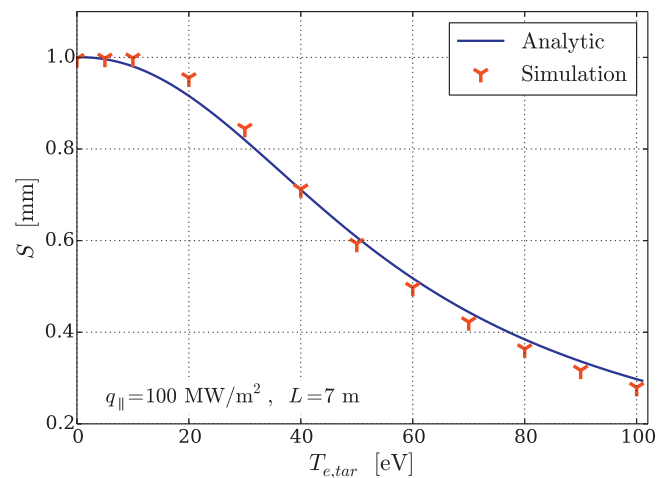


Fig. 1. Modelling results of the divertor broadening S in dependence of the target electron temperature. Red symbols are the modelling results, the blue line shows the analytic result using the two point model and assuming constant parallel heat flux density [11]. (For interpretation of the references to colour in this figure legend, the reader is referred to the web version of this article.)

that at high target temperatures (> 30 eV) the divertor broadening can be described by a power law, for low temperatures however S does not diverge, as would be expected for a power law with negative exponent, but it approaches a finite value. The analytic curve is obtained by integrating the square root of the ratio of the perpendicular and parallel heat diffusivity along the divertor leg [11]. For the temperature profile along the divertor leg the two point model is used assuming a constant parallel heat flux density.

$$S = \int_0^{l_x} \sqrt{\frac{\chi_{\perp}}{\chi_{\parallel}}} dl \quad (7)$$

For constant diffusivities Eq. (5) is reproduced. The reason why S is approaching a finite value is found in the integral, even for a target temperature of zero, the temperature in the divertor volume is still not zero. In absence of volume dissipation, the average temperature in the divertor is not reduced to zero for zero target temperatures, allowing only for a finite perpendicular diffusion due to the remaining parallel diffusivity, resulting in a finite divertor broadening S .

The results suggest that this approximation is only valid for high divertor temperatures [11]. For low $T_{e,tar}$ the temperature at the divertor target is not anymore a good qualifier for the divertor volume. Modelling shows that for low divertor temperatures, where the power law scalings [3,5] diverge, the divertor power spreading S approaches a finite value. This is understood since, without volume dissipation, only part of the divertor volume is cold, because the temperature gradient along the field line is large for low target temperatures. Due to this the power law scalings [3,5] cannot just be extrapolated towards low target electron temperatures. To further increase S the whole divertor volume needs to be cooled by volume dissipation e.g. using impurity seeding [12].

3. In/out asymmetry of the power fall-off length

Most of the studies on the power fall-off length λ_q have concentrated on the outer divertor target with the ion grad B drift direction towards the active X-point in deuterium. Recent studies on ASDEX Upgrade have extended this to both the inner and outer divertor target [4] also including hydrogen and helium as main ion species [5]. The following results were reported for deuterium as main ion species. For the open divertor configuration in ASDEX Upgrade it was found that the in/out asymmetry of the power fall-off

length is independent on the electron density but is described by the triangularity of the plasma for [4] which is in line with the assumption that vertical drifts are influencing λ_q [13]. It was found that λ_q is always smaller for the inner compared to the outer divertor target. For the closed configuration a similar in/out asymmetry is observed for low densities with a strong increase of the ratio $\lambda_{q,i}/\lambda_{q,o}$ with density, with $\lambda_{q,i}$ becoming larger than $\lambda_{q,o}$ until the inner divertor power detaches [5], in this case meaning that the power density is below 100 kWm^{-2} . Most notably the inner divertor power detaches before significant volume dissipation occurs in the divertor region. The increasing $\lambda_{q,i}$ decreases the parallel heat flux density $q_{\parallel,0}$ for constant total power P_{div} . It is concluded that the detachment of the inner divertor is accelerated by the increase of $\lambda_{q,i}$. The same observation was made for hydrogen but differences were found for helium [5].

3.1. Measurements

In this paper the density range covered by the measurements has been increased compared to the study made in [5]. The data presented here is obtained in attached low to medium recycling divertor conditions, where volume dissipation is negligible, up to power detachment where the heat flux density on the divertor target is below 100 kWm^{-2} . For the outer divertor target data using hydrogen, deuterium and helium as main ion is available, for the inner target only deuterium and helium is available.

It is found for the outer divertor target that hydrogen and deuterium behave similar with $\lambda_{q,o}$ exhibiting no density dependence and for helium showing a weak increase of $\lambda_{q,o}$ with increasing density. For the inner divertor target a strong increase of $\lambda_{q,i}$ is observed with increasing density, with $\lambda_{q,i}$ having a smaller absolute value in helium compared to deuterium. The limited density range could explain the observation in [5] that $\lambda_{q,i}$ does not increase strongly with increasing density, namely the density was not high enough. Using non linear regressions the following scalings for $\lambda_{q,o}$ [mm] are found for the outer divertor.

$$\lambda_{q,o,H} = 1.47 \cdot \frac{n_{e,edge}^{-0.05}}{B_{pol}^{0.73}} \quad (8)$$

$$\lambda_{q,o,D} = 1.33 \cdot \frac{n_{e,edge}^{0.10}}{B_{pol}^{0.73}} \quad (9)$$

$$\lambda_{q,o,He} = 1.52 \cdot \frac{n_{e,edge}^{0.49}}{B_{pol}^{0.73}} \quad (10)$$

For the regression, data for all three main ions has been used. The same exponent of B_{pol} [T] has been used in the regression for all three main ions, resulting in an exponent of -0.73 obtained by the regression. The pre factor and the exponent for the electron density $n_{e,edge}$ [10^{19} m^{-3}] have been used independently for each main ion. The dependence on B_{pol} is similar to the dependence found for H-Mode [14] with about twice the absolute size of $\lambda_{q,o}$ in L-Mode compared to H-Mode. For hydrogen and deuterium the density dependence is close to zero and for helium the density dependence is close to a square root dependence. The regression results for the outer divertor target are shown in Fig. 2.

One possible reason for the different density dependence of $\lambda_{q,o}$ in hydrogen/deuterium compared to helium could be the different recycling behaviour in the outer divertor.

For the inner divertor the exponent of B_{pol} has been set fixed to the exponent obtained for the outer divertor target of -0.73 since less data is available due to the limited operational space where the inner divertor is attached in L-Mode. The pre factor for deuterium and helium have been set independently as well as the ex-

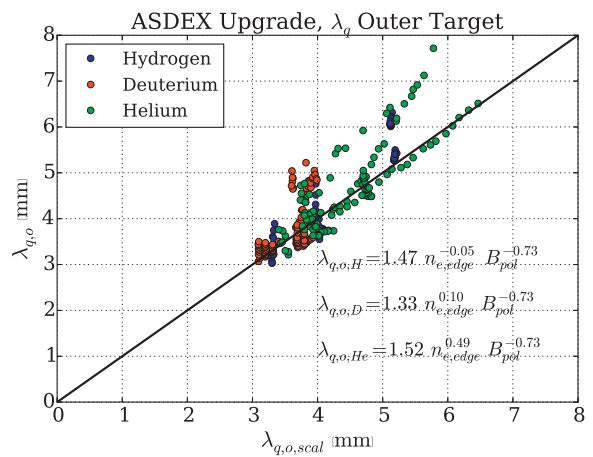


Fig. 2. Regression results for $\lambda_{q,o}$ on the outer divertor target for hydrogen, deuterium and helium.

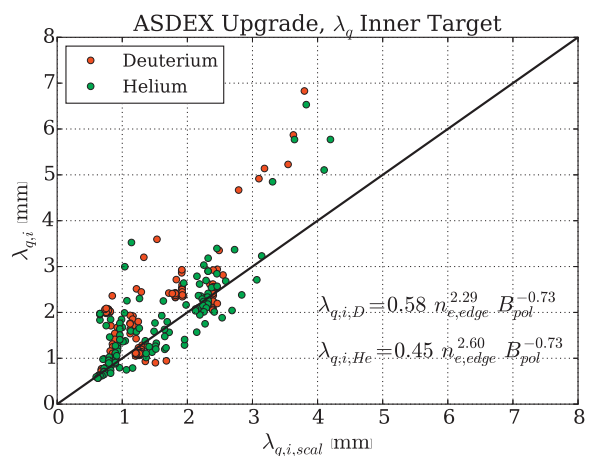


Fig. 3. Regression results for $\lambda_{q,i}$ on the inner divertor target for deuterium and helium.

ponent for $n_{e,edge}$. The results are:

$$\lambda_{q,i,D} = 0.58 \cdot \frac{n_{e,edge}^{2.29}}{B_{pol}^{0.73}} \quad (11)$$

$$\lambda_{q,i,He} = 0.58 \cdot \frac{n_{e,edge}^{2.60}}{B_{pol}^{0.73}} \quad (12)$$

For both deuterium and helium a more than square dependence of $\lambda_{q,i}$ on $n_{e,edge}$ is found. The regression results for the inner divertor target are shown in Fig. 3.

It is seen that for $\lambda_{q,i,scal} > 3 \text{ mm}$ the measured $\lambda_{q,i}$ is significantly larger than the values predicted by the scaling. This could indicate that for higher densities the edge electron density of the plasma is not a valid qualifier for the divertor conditions anymore. Considering the scatter of the data it is possible that an additional, yet to be determined, parameter is influencing $\lambda_{q,i}$.

Using these results the density dependence of the in/out asymmetry $\lambda_{q,i}/\lambda_{q,o}$ is found as.

$$\frac{\lambda_{q,i,D}}{\lambda_{q,o,D}} \propto n_{e,edge}^{2.19} \quad (13)$$

$$\frac{\lambda_{q,i,He}}{\lambda_{q,o,He}} \propto n_{e,edge}^{2.11} \quad (14)$$

The density dependence of $\lambda_{q,i}/\lambda_{q,o}$ is close to quadratic for both deuterium and helium.

It is notable that despite the difference in density dependence the data, especially for the outer divertor target, is described by the same parametric dependence.

3.2. Interpretation

Assuming vertical drifts are responsible for the power fall-off length λ_q [1,4,5,13] the following relation is found:

$$\lambda_q = \frac{2T}{v_{\parallel} e Z B_{pol} R} a \cdot (1 \pm \delta) \quad (15)$$

Where T is the upstream temperature, v_{\parallel} the parallel flow velocity in the scrape-off layer, Z the effective charge, B_{pol} the poloidal magnetic field, R the major radius, a the minor radius and δ the triangularity of the plasma. The ratio $\lambda_{q,i}/\lambda_{q,o}$ is found as:

$$\frac{\lambda_{q,i}}{\lambda_{q,o}} = \frac{1 - \delta}{1 + \delta} \cdot \frac{v_{\parallel,o}}{v_{\parallel,i}} \quad (16)$$

For low recycling divertor conditions it is assumed that the divertor acts as a perfect particle sink and that the parallel flow velocities $v_{\parallel,i} \approx v_{\parallel,o}$. Under this assumption $\lambda_{q,i}/\lambda_{q,o}$ is only dependent on δ which is observed for the open divertor configuration [4] and for the closed divertor configuration in low recycling conditions. For medium to high recycling divertor conditions the assumption that the divertor is a perfect particle sink is not applicable anymore which could explain the observed change of $\lambda_{q,i}/\lambda_{q,o}$ for the closed divertor configuration with increasing density.

For the closed configuration in ASDEX Upgrade the inner divertor is currently more optimized to accumulate a high density compared to the outer divertor. This could be the reason why the strong increase of λ_q is only observed on the inner target. For helium the observation is different here λ_q increases with increasing density for the outer divertor target. The different recycling behaviour of helium and hydrogen/deuterium could be the reason for the observed difference in the density dependence of λ_q . So far no clear answer can be given of why the power fall-off length behaves different in helium compared to hydrogen/deuterium. The processes leading to the recycling of particles in the divertor could be different due to e.g. different charge exchange cross sections or in the different mean free path of particles which lead to ballistic/diffusive transport. Detailed modelling of the divertor conditions in helium and hydrogen/deuterium could help to understand the underlying differences.

4. Magnetic perturbation

The application of external magnetic perturbation (MP) is studied as a tool to reduce the heat impact of ELMs onto the plasma facing components [15–17]. Exploiting the high resolution IR thermography [6] and the ability to rotate the external MP in ASDEX Upgrade [18,19] the full 2D heat flux pattern on the divertor target has been measured in L-Mode conditions. A detailed overview of the experiments and the results is given in [20], a brief summary is shown here. The main experiments have been conducted with a toroidal magnetic field of $B_{tor} = -2.5$ T and a plasma current of $I_p = 0.8$ MA with a toroidal mode number of the perturbation of $n = 2$ in resonant and non-resonant configuration with low to medium recycling divertor conditions, with a current in the perturbation coils of 1.0 kA. In presence of the MP a non axisymmetric heat flux pattern is observed on the divertor target. The local heat flux densities can both be lower and higher compared to the axisymmetric case without MP. Toroidal averaging over the 2D heat flux pattern recovers a heat flux profile which is equivalent to the axisymmetric case. Most notably λ_q obtained from the averaged heat flux profile is the same as for the reference case without MP within the uncertainty. Fig. 4 shows the poloidal heat flux profile

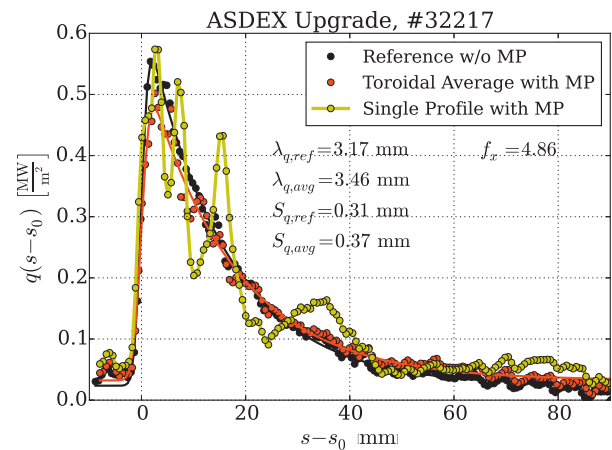


Fig. 4. Heat flux profile on the outer divertor target of ASDEX Upgrade with and w/o magnetic perturbation.

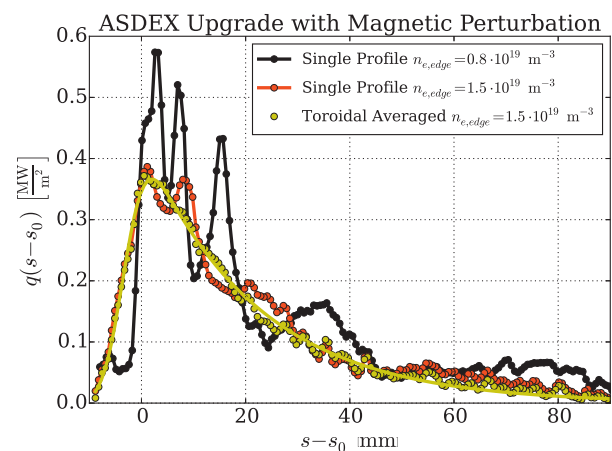


Fig. 5. Characteristic lobe pattern in the heat flux profile on the outer divertor target for different edge electron densities.

with MP (yellow), without MP (black) and the toroidal averaged heat flux profile with MP (red).

It is observed that λ_q and S do not vary in the presence of MP compared to the reference w/o MP within the uncertainty of the measurement. The characteristic of the 2D pattern is reduced with increasing density. Fig. 5 shows the heat flux pattern with MP for different upstream edge electron densities. It is seen that for higher density (red) the excursion of the characteristic lobe structure is reduced compared to the case with lower density (black). The toroidal average again reproduces a smooth profile that is described by λ_q and S .

It is thought that an increased power spreading S with higher density is mitigating the strength of the 2D heat flux pattern, approaching an axisymmetric profile for large S . This could ease the requirements to rotate the external MP to prevent local overheating in large devices like ITER.

5. Conclusion

It is found that the power spreading in the divertor region is described by the competition of perpendicular heat diffusion and parallel electron conduction. The ion gyro radius needs to be taken into account for large divertor temperatures (>30 eV).

For low recycling divertor conditions an in/out asymmetry of the power fall-off length λ_q in a closed divertor geometry is observed which is similar to early findings made in open configuration [4]. These findings are in line with the drift based model for

λ_q [13] which predicts an asymmetry of $\lambda_{q,i}/\lambda_{q,o}$ which is dependent on the triangularity of the plasma. For increasing densities with increasing divertor recycling the ratio $\lambda_{q,i}/\lambda_{q,o}$ is strongly increasing for both deuterium and helium. It is found that for both deuterium and helium $\lambda_{q,i}$ strongly increases with increasing density. For the outer divertor target a weak increase of $\lambda_{q,o}$ is observed for helium and no significant density dependence of $\lambda_{q,o}$ is found for hydrogen and deuterium.

One possible explanation for this observation is the decreasing parallel flow velocity $v_{||}$ in the scrape-off layer. The drift based model predicts an increase of λ_q for decreasing $v_{||}$. The observed increase of λ_q could be due to a decrease of $v_{||}$ due to the increased recycling in the divertor region with increasing density. The in/out asymmetry could be due to the higher degree of optimization of the inner divertor target compared to the outer divertor target and the resulting better divertor compression of the inner divertor.

Acknowledgement

This work has been carried out within the framework of the EUROfusion Consortium and has received funding from the Euratom research and training programme 2014–2018 under grant agreement No 633053. The views and opinions expressed herein do not necessarily reflect those of the European Commission.

References

- [1] T. Eich, et al., *Phys. Rev. Lett.* 107 (2011) 215001.
- [2] B. Sieglin, et al., *Plasma Phys. Controlled Fusion* 55 (12) (2013) 124039.
- [3] A. Scarabosio, et al., *J. Nucl. Mater.* (2014).
- [4] M. Faitsch, et al., *Plasma Phys. Controlled Fusion* 57 (7) (2015) 075005.
- [5] B. Sieglin, et al., *Plasma Phys. Controlled Fusion* 58 (5) (2016) 055015.
- [6] B. Sieglin, et al., *Rev. Sci. Instrum.* 86 (11) (2015).
- [7] M.A. Makowski, et al., *Phys. Plasmas* (1994–present) 19 (5) (2012) 056122.
- [8] M. Wischmeier, et al., *J. Nucl. Mater.* 415 (1, Supplement) (2011) S523–S529. Proceedings of the 19th International Conference on Plasma-Surface Interactions in Controlled Fusion.
- [9] A. Kukushkin, et al., *Fusion Eng. Des.* 86 (12) (2011) 2865–2873.
- [10] D. Coster, *J. Nucl. Mater.* 415 (1, Supplement) (2011) S545–S548. Proceedings of the 19th International Conference on Plasma-Surface Interactions in Controlled Fusion.
- [11] D. Nille, et al., arXiv:1610.04148 (2016).
- [12] A. Kallenbach, et al., *Plasma Phys. Controlled Fusion* 58 (4) (2016) 045013.
- [13] R. Goldston, et al., *Nucl. Fusion* 52 (1) (2012) 013009.
- [14] T. Eich, et al., *Nucl. Fusion* 53 (9) (2013) 093031.
- [15] W. Suttrop, et al., *Fusion Eng. Des.* 88 (68) (2013) 446–453. Proceedings of the 27th Symposium On Fusion Technology (SOFT-27); Lige, Belgium, September 24–28, 2012.
- [16] T. Evans, *J. Nucl. Mater.* 438, Supplement (2013) S11–S18. Proceedings of the 20th International Conference on Plasma-Surface Interactions in Controlled Fusion Devices.
- [17] A. Thornton, et al., *J. Nucl. Mater.* 463 (2015) 723–726. PLASMA-SURFACE INTERACTIONS 21 Proceedings of the 21st International Conference on Plasma-Surface Interactions in Controlled Fusion Devices Kanazawa, Japan May 26–30, 2014.
- [18] W. Suttrop, et al., *Fusion Eng. Des.* 84 (26) (2009) 290–294. Proceeding of the 25th Symposium on Fusion Technology (SOFT-25).
- [19] M. Teschke, et al., *Fusion Eng. Des.* 96–97 (2015) 171–176. Proceedings of the 28th Symposium On Fusion Technology (SOFT-28).
- [20] M. Faitsch, et al., Nuclear Materials and Energy, PSI 2016 Conference Proceedings, submitted.